Appl. Phys. A 79, 439–442 (2004)
DOI: 10.1007/s00339-004-2707-x

Applied Physics A
Materials Science & Processing

B. LEI
C. LI
D. ZHANG
T. TANG
C. ZHOU✉

Tuning electronic properties of In_2O_3 nanowires by doping control

Department of EE – Electrophysics, University of Southern California, Los Angeles, CA 90089, USA

Received: 6 February 2004/Accepted: 9 February 2004
Published online: 23 March 2004 •

ABSTRACT We present two effective routes to tune the electronic properties of single-crystalline In_2O_3 nanowires by controlling the doping. The first method involves using different O_2 concentrations during the synthesis. Lightly (heavily) doped nanowires were produced by using high (low) O_2 concentrations, respectively, as revealed by the conductances and threshold voltages of nanowire-based field-effect transistors. Our second method exploits post-synthesis baking, as baking heavily doped nanowires in ambient air led to suppressed conduction and a positive shift of the threshold voltage, whereas baking lightly doped nanowires in vacuum displayed the opposite behavior. Our approaches offer viable ways to tune the electronic properties of many nonstoichiometric metal oxide systems such as In_2O_3, SnO_2, and ZnO nanowires for various applications.

PACS 85.35.-p

Recent interest in low-dimensional materials such as nanotubes and nanowires is motivated by the push of miniaturization of electronic and optoelectronic devices and a need to understand the fundamentals of nanoscale chemistry and physics [1, 2]. Recently, In_2O_3 nanowires as an *n*-type semiconductor have been attracting increasingly more attention due to their distinctive optical and electronic properties. Following the successful synthesis of single-crystalline In_2O_3 nanowires [3, 4], their properties such as electronic transport characteristics [5], chemical sensing [6], and photoluminescence [4, 7] have been under intensive investigation. The doping concentration of the In_2O_3 nanowires is determined by the oxygen-vacancy level [8] and very often dominates the performance of such nanowire devices. Tuning the electronic properties of In_2O_3 nanowires by doping control is therefore indispensable for various studies and applications. In this study, we present two effective routes to tune the doping concentration of In_2O_3 nanowires, which subsequently led to nanowire transistors with dramatically different electronic properties. Our method has great potential to be generalized to other oxide nanowires such as SnO_2 and ZnO.

Our first approach is called synthetic doping control, with which nanowires were synthesized by using different concentrations of O_2 in Ar during the nanowire synthesis. This led to different oxygen-vacancy concentrations in the nanowires, thus lending us a way to tune the nanowire electronic properties. The second method is called post-synthesis baking, which was first demonstrated for SnO_2 nanobelt transistors [9]. With this technique nanowires were baked in either air or vacuum to reduce or enrich the oxygen-vacancy concentrations, respectively.

✉ Fax: +1-213/740-8677, E-mail: chongwuz@usc.edu

Single-crystalline In_2O_3 nanowires were synthesized by a laser ablation process described previously [3]. An InAs target was placed at the upstream end of a quartz-tube furnace, and a Si/SiO_2 substrate decorated with mono-dispersed 10-nm gold clusters was loaded into the furnace with an optimized distance from the target and used to collect the final products. The laser beam was introduced through a view-port and used to ablate the target to generate the indium (In) vapor, which was carried downstream by a constant flow of argon (150 sccm) mixed with a trace amount of oxygen. Our growth follows the well-known vapor–liquid–solid mechanism, as the indium vapor first diffuses into the gold catalyst particles to form a liquid alloy drop. Continued supply of indium brought the In/Au alloy beyond supersaturation, followed by the outgrowth of indium and reaction with ambient oxygen to form single-crystalline In_2O_3 nanowires. No arsenic has been detected in our nanowires using energy-dispersive X-ray spectroscopy (EDS), which is understandable as oxygen is a lot more reactive than arsenic. These oxide nanowires are usually *n*-type doped due to oxygen vacancies, and the vacancy concentration should be directly linked to the oxygen concentration in the reaction system. For synthetic doping control, we used two different concentrations of oxygen in argon: 0.017% (denoted condition 1) and 0.04% (denoted condition 2), both of which produced nanowires exhibiting high conduction and strong gate dependence, making them ideal for various applications. Even higher or lower oxygen concentrations were also used for

nanowire synthesis; however, transistors based on such nanowires exhibited either low conduction (doping too low) or threshold voltages below −30 V (doping too high), making them less useful for practical applications. The as-synthesized In_2O_3 nanowires were dispersed onto a degenerately doped Si wafer covered with 500-nm SiO_2. Photolithography and Ti/Au deposition were subsequently performed to pattern the source and drain electrodes to contact individual nanowires. The Si substrate was used as a back gate in our following electronic measurements. Figure 1a (inset) shows a scanning electron microscope (SEM) micrograph of a typical device made in this way, where a nanowire bridging the source and drain electrodes can be clearly seen. Our nanowire field-effect transistors (FETs) typically have channel width ∼ 10 nm (defined by the nanowire diameter) and channel length ∼ 2–3 μm.

For synthetic doping control studies, two families of field-effect transistors (denoted groups #1 and #2) were fabricated based on nanowires synthesized under conditions 1 and 2, respectively. This was followed by thorough electronic characterization to determine the conductance and the doping level of these nanowires. All the electronic measurements were performed at room temperature under ambient conditions. For sample group #1 produced with 0.017% O_2 in Ar, altogether 27 nanowire devices were carefully studied. Figure 1a shows a family of current–voltage (I–V) curves of a typical device of group #1 under different gate biases (V_g). Five curves at $V_g =$ 0 V, −10 V, −15 V, −20 V, and −25 V are displayed in this figure. With the gate voltage varying from 0 V to −25 V, the conductance was progressively suppressed, indicating n-type semiconductor behavior. The linear conductance of this device can be derived from the slopes of I–V curves at $V = 0$ V, and was found to be reduced from 4.43×10^{-6} S (2.26×10^5 Ω) at $V_g =$ 0 V to 2.88×10^{-10} S (3.47×10^9 Ω) at $V_g = -25$ V, indicating an on/off ratio as high as 10^4. The lower inset in Fig. 1a displays an I–V_g plot of the device with the drain–source bias $V = 0.05$ V, and a threshold gate voltage (V_{th}) can be determined to be ∼ −28 V. The doping concentration along the wire can be estimated using the formula $n \equiv Q/eL = 2\pi\varepsilon\varepsilon_0 V_{th}/[eln(2h/r)]$ [10], with Q being the total charge along the wire, e the electron charge, ε_0 the vacuum dielectric constant, L and r the length and radius of the nanowire, h the thickness of the SiO_2 layer, and ε the relative dielectric constant of SiO_2. n is therefore calculated to be 7.16×10^7 cm^{-1} by substituting the data $V_{th} = -28$ V, $r =$ 5 nm, $h = 500$ nm, and $\varepsilon = 3.9$. This value corresponds to 7.16 electrons per nanometer, indicating that the nanowire is heavily doped with oxygen vacancies. The mobility of the carriers can be further deduced from the transconductance of the FET. In the linear regime, it is given by $dI/dV_g = n\mu eV/(V_{th}L)$. We get $\mu = 111.5$ cm^2/V s with $V = 0.05$ V, $L = 3$ μm, and $dI/dV_g = 7.6 \times 10^{-9}$ A/V. To fully illustrate the doping control effect, all 27 devices from group #1 were thoroughly characterized, and a histogram of the threshold gate voltage distribution is plotted in Fig. 1b. One can clearly see that the majority of the devices have V_{th} between −25 V and −30 V, even though a small number of devices with higher or lower V_{th} were also observed. A Gaussian fit of the distribution reveals a mean threshold voltage of −28 V.

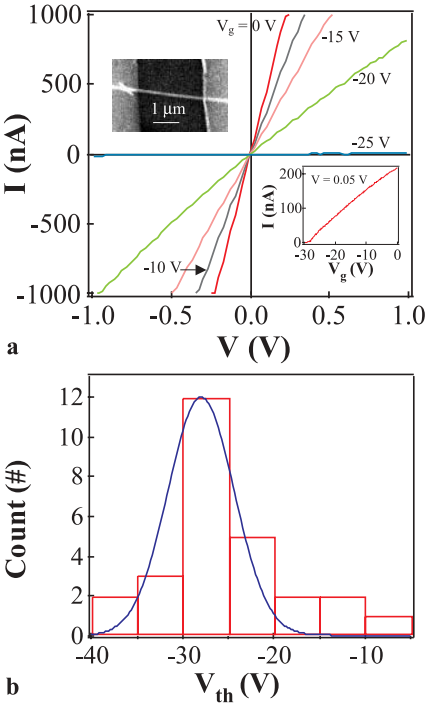

FIGURE 1 Electronic properties of In_2O_3 nanowires synthesized with 0.017% O_2 in Ar. **a** Gate-dependent I–V curves recorded at room temperature. *Lower inset*: I–V_g curve measured at $V = 50$ mV. *Upper inset*: SEM micrograph showing an In_2O_3 nanowire between two electrodes. **b** Histogram of the threshold voltage of 27 nanowire transistors showing a mean value of −28 V

For sample group #2 synthesized with 0.04% O_2 in Ar, altogether 35 devices were carefully characterized via I–V and I–V_g measurements. Figure 2a shows six I–V curves at $V_g =$ 0 V, −2 V, −4 V, −6 V, −8 V, and −10 V from a typical device. While a strong gate dependence was also observed, these I–V curves are highly nonlinear with a zero-bias conductance of 6.57×10^{-7} S (1.52×10^6 Ω) at $V_g =$ 0 V, as compared to 4.43×10^{-6} S for the device shown in Fig. 1a. The inset of Fig. 2b shows the I–V_g curve taken at $V = -0.2$ V, showing a threshold gate voltage V_{th} of −10 V. The doping concentration and the carrier mobility were deduced to be 2.56×10^7 cm^{-1} and 279.05 cm^2/V s, respectively, following the aforementioned method. Figure 2b shows a histogram of the threshold voltage for 35 devices from sample group #2, and the Gaussian fit reveals a mean value of −10 V, as compared to a mean value of −28 V for sample group #1.

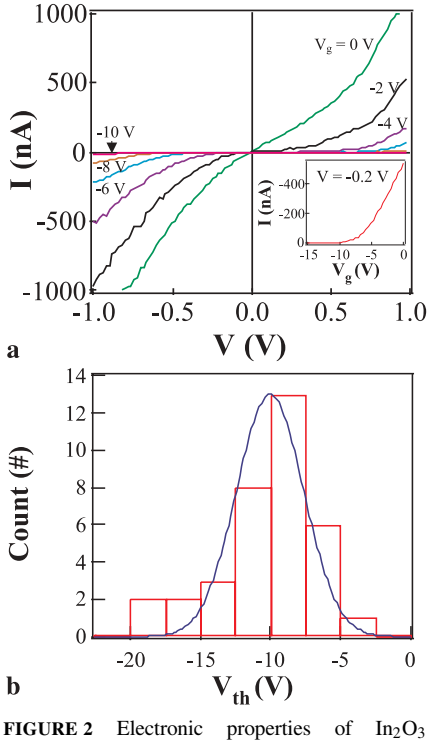

FIGURE 2 Electronic properties of In_2O_3 nanowires synthesized with 0.04% O_2 in Ar. **a** Gate-dependent I–V curves recorded at room temperature. *Lower inset*: I–V_g curve measured at $V = -0.2$ V. **b** Histogram of the threshold voltage of 35 nanowire transistors showing a mean value of −10 V

This significant discrepancy unambiguously confirms the feasibility of the synthetic doping control approach as, relatively speaking, devices from group #1 can be considered heavily doped with typical $n = 7.16 \times 10^7\,\mathrm{cm}^{-1}$ and devices from group #2 can be considered lightly doped with typical $n = 2.56 \times 10^7\,\mathrm{cm}^{-1}$. We attribute this doping control effect to the formation of oxygen vacancies during the nanowire synthesis [11]. The oxygen vacancies act as doubly charged donors providing electrons to the conduction band. Lower O_2 concentration leads to a higher population of oxygen vacancies and consequently high conductance, whereas higher O_2 concentration leads to a lower population of oxygen vacancies as well as low conductance.

Compared to the synthetic doping control approach, post-synthesis baking offers a tantalizing alternative to tune the nanowire electronic properties after the synthesis. By baking samples under either oxygen-rich (e.g. ambient air) or oxygen-deficient (e.g. vacuum) ambient conditions, oxygen can diffuse either into or out of the nanowires, and thus one can controllably reduce or increase the oxygen-vacancy concentration inside the nanowires. Figure 3a shows the I–V curves at $V_g = 0$ V recorded before and after baking a heavily doped nanowire device in ambient air. The I–V curve recorded before annealing is linear with a high conduction of 974.98 nA at 0.5 V. After baking, the device exhibited a current of 0.0285 nA at the same source–drain voltage, indicating a decrease in conductance of up to four orders of magnitude. Furthermore, I–V_g curves were also recorded at a fixed source–drain bias of -0.2 V before and after annealing, as shown in Fig. 3b. A pronounced positive shift of the threshold voltage from -30 V (before baking) to 2 V (after baking) was observed, accompanied with a significant suppression in conductance at $V_g = 0$ V. From these data, the change of carrier concentration can be estimated by $C\Delta V_{th}/eL \sim -8.06 \times 10^7\,\mathrm{cm}^{-1}$, where ΔV_{th} is the shift of the threshold voltage, C is the capacitance of the nanowire estimated to be 1.21×10^{-16} F, and L is the nanowire length (~ 3 μm). This reduction in the carrier concentration caused the drastic suppression in conductance.

Similar experiments were performed for a lightly doped nanowire device, which was baked at 200 °C for 10 min in high vacuum, i.e. an oxygen-deficient environment. Figure 4a shows the I–V curves measured at $V_g = -3$ V and Fig. 4b shows the I–V_g curves measured at $V = -0.4$ V before and after baking in vacuum. A pronounced increase in conductance was observed up to two orders of magnitude at $V = 0.5$ V after baking the device in vacuum, in addition to a shift of the threshold gate voltage from -2 V to -7 V. The change of carrier concentration can be estimated to be $\sim 1.26 \times 10^7\,\mathrm{cm}^{-1}$, following the method described above. In sharp contrast to the heavily doped nanowire device shown in Fig. 3, this device exhibited a pronounced increase in conductance due to an increase in the carrier concentration. We attribute these observations to the change of oxygen-vacancy concentrations in the nanowires. Baking in ambient air leads to oxygen diffusing into the nanowires, which can fill up the oxygen-vacancy sites and thus cause a drastic reduction in the free-electron concentration, as confirmed by the observed suppression in conductance. In contrast, baking in vacuum leads to the diffusion of oxygen atoms in normal lattice sites to the gaseous state, thus generating oxygen vacancies as electron donors and causing the observed increase in conductance. This post-synthesis baking approach is especially effective for nanowires due to their ultra-high surface-to-volume ratios, as the surface not only absorbs or desorbs oxygen molecules but also provides a large window for oxygen diffusion into or out of the nanowire.

In summary, we have presented two effective routes to tune the electronic properties of In_2O_3 nanowire transistors by controlling the doping concentration. By synthesizing nanowires with two different oxygen concentrations (0.017% vs. 0.04%), we have produced either heavily or lightly doped nanowires ($7.16 \times 10^7\,\mathrm{cm}^{-1}$ vs. $2.56 \times 10^7\,\mathrm{cm}^{-1}$) with dramatically different conduction levels and threshold voltages. Furthermore, annealing heavily doped nanowires in ambient air led to suppressed conduction and a positive shift of the threshold voltage, whereas annealing lightly doped nanowires in vacuum displayed the opposite behavior. Our approaches offer viable ways to tune the

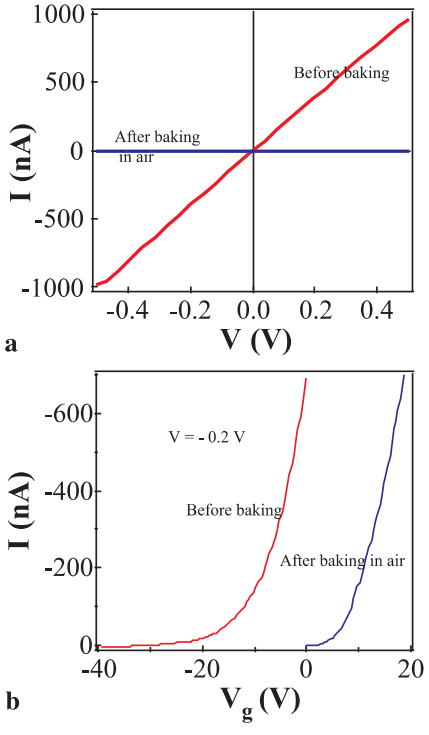

FIGURE 3 **a** I–V curves and **b** I–V_g curves of a heavily doped nanowire transistor taken before and after baking in ambient air at 200 °C

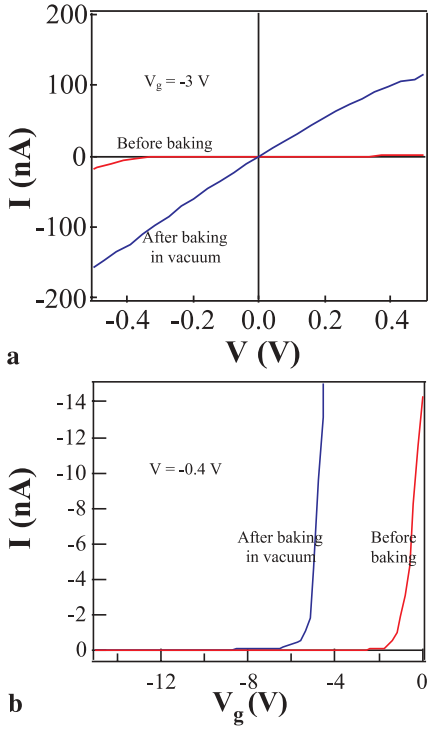

FIGURE 4 **a** I–V curves and **b** I–V_g curves of a lightly doped nanowire transistor taken before and after baking in vacuum at 200 °C

electronic properties of many nonstoichiometric metal oxide systems such as In_2O_3, SnO_2, and ZnO nanowires for various applications.

ACKNOWLEDGEMENTS The authors thank Dr. J. Han and Dr. M. Meyyapan of NASA Ames Research Center for valuable technical discussions. This work is supported by USC, NASA Contract No. NAS2-99092, an NSF CAREER award, the NSF CENS program, the SRC/MARCO program, and the Norris Foundation.

REFERENCES

1 M.A. Reed, T. Lee: *Molecular Nanoelectronics* (American Scientific Publishers, 25659 North Lewis Way, Stevenson Ranch, California 91381-1439, USA 2003)
2 M.S. Gudiksen, J. Wang, C.M. Lieber: J. Phys. Chem. B **106**, 4036 (2002)
3 C. Li, D. Zhang, S. Han, X. Liu, T. Tang, W. Jin, C. Zhou: Adv. Mater. **15**, 143 (2003)
4 X.S. Peng, G.W. Meng, J. Zhang, X.F. Wang, Y.W. Wang, C.Z. Wang, L.D. Zhang: J. Mater. Chem. **12**, 1602 (2002)
5 D. Zhang, C. Li, S. Han, X. Liu, T. Tang, W. Jin, C. Zhou: Appl. Phys. Lett. **82**, 112 (2003)
6 C. Li, D. Zhang, X. Liu, S. Han, T. Tang, J. Han, C. Zhou: Appl. Phys. Lett. **82**, 1613 (2003)
7 M.J. Zheng, L.D. Zhang, G.H. Li, X.Y. Zhang, X.F. Wang: Appl. Phys. Lett. **79**, 839 (2001)
8 J.R. Bellingham, A.P. Mackenzie, W.A. Phillips: Appl. Phys. Lett. **58**, 2506 (1991)
9 M.S. Arnold, P. Avouris, Z. Pan, Z.L. Wang: J. Phys. Chem. B **107**, 659 (2003)
10 R. Martel, T. Schmidt, H.R. Shea, T. Hertel, P. Avouris: Appl. Phys. Lett. **73**, 2447 (1998)
11 M. Bender, N. Katsarakis, E. Gagaoudakis, E. Hourdakis, E. Douloufakis, V. Cimalla, G. Kiriakidis: J. Appl. Phys. **90**, 5382 (2001)